



## Short communication

## Effect of pore diameter of wormholelike mesoporous carbon supports on the activity of Pt nanoparticles towards hydrogen electrooxidation

Shuqin Song<sup>a,\*\*</sup>, Shibin Yin<sup>a</sup>, Zhenghui Li<sup>b</sup>, Pei Kang Shen<sup>a</sup>, Ruowen Fu<sup>b</sup>, Dingcai Wu<sup>b,\*</sup><sup>a</sup> State Key Laboratory of Optoelectronic Materials and Technologies, School of Physics and Engineering, Sun Yat-sen University, Xingang West Road 135, Guangzhou 510275, China<sup>b</sup> Materials Science Institute, PCFM Laboratory, School of Chemistry and Chemical Engineering, Sun Yat-sen University, Guangzhou 510275, China

## ARTICLE INFO

## Article history:

Received 4 September 2009

Received in revised form 5 October 2009

Accepted 6 October 2009

Available online 13 October 2009

## Keywords:

Wormholelike mesoporous carbons

Pt nanoparticles

Pore diameter

Hydrogen electrooxidation

## ABSTRACT

Pt nanoparticles are successfully deposited on wormholelike mesoporous carbons (WMCs) using a pulse microwave-assisted polyol method. WMCs with two different pore diameters are used. The particle size of Pt on both supports is identical, about 3 nm. It has been found that Pt utilization efficiency is very low when the pore diameter of WMCs ( $D_p$ ) is equal to the diameter of Pt nanoparticles ( $D_{Pt}$ ). However, in the case that  $D_p$  is more than twice  $D_{Pt}$ , the electrochemical surface area and Pt utilization efficiency are dramatically enhanced, and in turn, hydrogen electrooxidation activity is greatly improved.

© 2009 Elsevier B.V. All rights reserved.

## 1. Introduction

The high cost of Pt and its scarce resources are one of the key issues hindering the development and commercialization of proton exchange membrane fuel cells (PEMFCs). To address this problem, much effort has been devoted to reduce Pt loading by increasing Pt utilization [1,2]. The Pt utilization enhancement can be accomplished through using Pt nanoparticles which can increase the surface-to-mass ratio and adopting conductive supporting materials with high specific surface area and desirable porous structure for Pt accessibility [3–5]. However, it is known that in electrochemical reactions, not all the geometric surface area can be involved into the electrocatalysis. Only a minority of Pt nanoparticles are electrochemically active while a majority of Pt nanoparticles are inaccessible to reactants [6]. For the support materials of electrocatalysts, it is of crucial importance to provide high surface area, excellent electronic conductivity, and suitable pore structure for the desirable mass transportation.

As known, carbon black Vulcan XC-72 is the commonly used support material. However, it is an essentially nonporous material and thus has a low surface area, leading to low utilization of Pt catalysts [7,8]. Recently, some porous carbon materials with high surface area, such as carbon cryogel with Brunner–Emmett–Teller

(BET) surface area of  $517 \text{ m}^2 \text{ g}^{-1}$  [3] and  $\text{PrO}_x$  decorated ordered mesoporous carbon with BET surface area of  $1330 \text{ m}^2 \text{ g}^{-1}$  [9], have been proven to be good support materials of Pt nanoparticles for hydrogen electrooxidation. However, there are few studies that specifically focus on the relationship between porous carbon supports' pore diameter and Pt nanoparticles' activity for hydrogen electrooxidation.

Herein we report the pore size dependence of accessibility of Pt nanoparticles supported on wormholelike mesoporous carbons (WMCs) with two types of pore diameters ( $D_p$ ) as follows: (a) 3.1 nm, which is equal to the diameter of Pt nanoparticles ( $D_{Pt}$ ), and (b) 8.5 nm, which is more than twice  $D_{Pt}$ . We found that the pore size effect is surprisingly decisive for the accessibility of Pt nanoparticles and consequently their utilization efficiency and electrocatalytic activity.

## 2. Experimental

WMCs with pore diameter of 3.1 and 8.5 nm (denoted as WMC-F0 and WMC-F4, respectively) [10] were adopted as the porous carbon support model. Their corresponding structure parameters are given in Table 1. WMCs supported Pt catalysts were synthesized by a modified pulse-microwave assisted polyol method [2]. The Pt loading was 20 wt% and the obtained catalysts were denoted as Pt/WMC-F0 and Pt/WMC-F4. In order to check whether the precursor has been reduced, we measured the Pt ion concentration in the mother solution and the result confirmed that the chloroplatinic acid was completely reduced.

\* Corresponding author. Tel.: +86 20 84112759; fax: +86 20 84115112.

\*\* Corresponding author. Tel.: +86 20 84113253; fax: +86 20 84113253.

E-mail addresses: stsssq@mail.sysu.edu.cn (S. Song), wudc@mail.sysu.edu.cn (D. Wu).

**Table 1**

Carbon supports' pore structure parameters and Pt nanoparticles' diameter and properties for Pt/WMC-F0 and Pt/WMC-F4.

Sample	$D_p$ (nm)	$S_{\text{BET}}^a$ ( $\text{m}^2 \text{g}^{-1}$ )	$D_{\text{Pt}}$ (nm)	$S_{\text{CSA}}$ ( $\text{m}^2 \text{g}^{-1}$ )	$S_{\text{ESA}}$ ( $\text{m}^2 \text{g}^{-1}$ )	$\eta_{\text{Pt}}$ (%)
Pt/WMC-F0	3.1	1372	3.1	90.4	3.5	3.9
Pt/WMC-F4	8.5	659	3.1	90.4	89.9	99.4

Note:  $D_p$  and  $S_{\text{BET}}$  are taken from [10] and  $D_{\text{Pt}}$  is obtained from XRD results.

<sup>a</sup>  $S_{\text{BET}}$ : BET surface area.

The prepared catalysts were characterized by an X-ray diffractometer using Cu K $\alpha$  radiation ( $\lambda = 0.15406$  nm) and a transmission electron microscope (TEM). Electrochemical measurements were conducted on an electrochemical workstation adopting a saturated calomel electrode (SCE) and a Pt foil as the reference electrode and the counter electrode, respectively. The working electrode was a glass carbon (GC) disk electrode ( $\varnothing = 5.0$  mm). The electrode was prepared by mixing 10.0 mg electrocatalyst, 1.8 mL ethanol and 0.2 mL Nafion solution (5 wt%). The catalyst ink was then quantitatively transferred onto the surface of the GC electrode and dried to obtain a catalyst thin film. The Pt loading was maintained to be  $25.5 \mu\text{g Pt cm}^{-2}$ . The catalysts were tested in  $0.1 \text{ mol L}^{-1}$  HClO $_4$ , deaerated with N $_2$  for electrochemical surface area measurement or saturated with H $_2$  for hydrogen electrooxidation. Without specification, the potential is referred to the reversible hydrogen electrode (RHE).

### 3. Results and discussion

Fig. 1(a) shows the X-ray diffraction (XRD) results of Pt/WMC-F0 and Pt/WMC-F4. As clearly displayed, both samples exhibit the typical characteristics of a crystalline Pt face centered cubic (fcc) structure. The fitted (220) plane (the inset of Fig. 1(a)) was used to calculate the average Pt particle size according to Scherrer formula, with the average particle size of 3.1 nm in both cases. Such a particle size value is supported by their TEM images ( $\sim 3$  nm, Fig. 1(b)). This allows one to eliminate the effect of Pt particle size and thus will be advantageous for the investigation of their pore diameter effect on Pt's electrochemical properties. Moreover, it can be seen from Fig. 1(b) that the Pt nanoparticles are uniformly dispersed on the pore surface of both WMCs. This indicates that though these two WMCs have different pore size, their high BET surface area as given in Table 1 provides

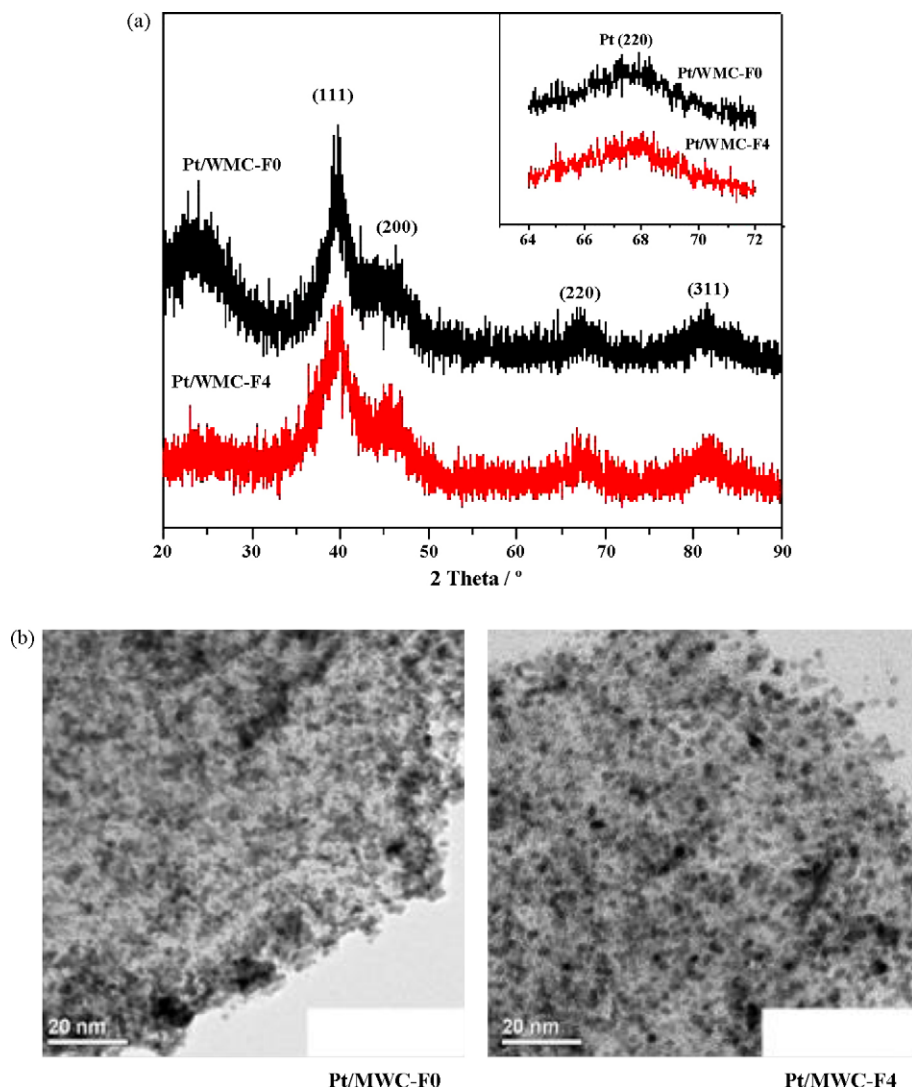


**Fig. 1.** Physico-chemical characterization of the as-prepared Pt supported on wormholelike mesoporous carbon materials with various pore size. (a) XRD spectra and their corresponding detailed Pt (220) peaks scanned at  $1^\circ \text{ min}^{-1}$  and (b) TEM images.

them with the desirable ability to disperse Pt nanoparticles very well.

Fig. 2 shows the cyclic voltammetric (CV) results of Pt/WMC-F0 and Pt/WMC-F4 in 0.1 mol L<sup>-1</sup> HClO<sub>4</sub>. The electrochemical surface area ( $S_{\text{ESA}}$ ) can be obtained by using Eq. (1) from the integrated charge in the hydrogen adsorption peak area in the CV curves in Fig. 2(a) and Pt poly-crystallite hydrogen adsorption constant (210  $\mu\text{C cm}^{-2}$  Pt). The chemical surface area ( $S_{\text{CSA}}$ ) and the Pt utilization efficiency ( $\eta_{\text{Pt}}$ ) can be calculated using Eqs. (2) and (3), respectively [11,12].

$$S_{\text{ESA}} [\text{m}^2 \text{ Pt/mg Pt}] = \text{charge} [\mu\text{C/cm}^2] / 210 [\mu\text{C/cm}^2 \text{ Pt}] \times \text{Pt loading} [\text{mg/cm}^2] \times 10^4 \quad (1)$$

$$S_{\text{CSA}} = 6 \times 10^4 / (\rho D_{\text{Pt}}) \quad (2)$$

$$\eta_{\text{Pt}} (\%) = S_{\text{ESA}} / S_{\text{CSA}} \times 100 \quad (3)$$

In Eq. (2),  $D_{\text{Pt}}$  is the average Pt particle size in  $\text{\AA}$  (from XRD result) and  $\rho$  is the density of Pt metal (21.4 g cm<sup>-3</sup>).

Based on the experimental results and above equations, the corresponding  $S_{\text{ESA}}$ ,  $S_{\text{CSA}}$  and  $\eta_{\text{Pt}}$  for both samples are obtained and summarized in Table 1. Clearly, Pt/WMC-F4 has an electrochemical surface area of 89.9 m<sup>2</sup> g<sup>-1</sup>, about 26 times as big as that of Pt/WMC-F0. Due to the same average Pt particle size, the Pt utilization efficiency gives the same tendency as the electrochemical surface area, with  $\eta_{\text{Pt}} = 99.4\%$  for Pt/WMC-F4 and  $\eta_{\text{Pt}} = 3.9\%$  for Pt/WMC-F0.

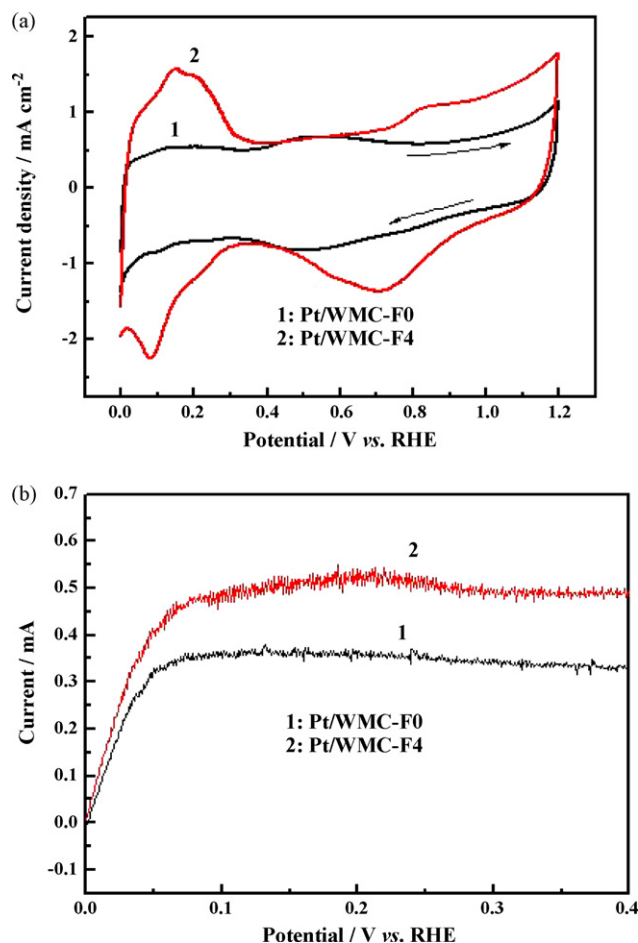


Fig. 2. (a) CV curves in deaerated 0.1 mol L<sup>-1</sup> HClO<sub>4</sub> at a scan rate of 20 mV s<sup>-1</sup>, and (b) hydrogen electrooxidation polarization curves in H<sub>2</sub> saturated 0.1 mol L<sup>-1</sup> HClO<sub>4</sub> over Pt/WMC-F0 and Pt/WMC-F4 at a scan rate of 5 mV s<sup>-1</sup>.

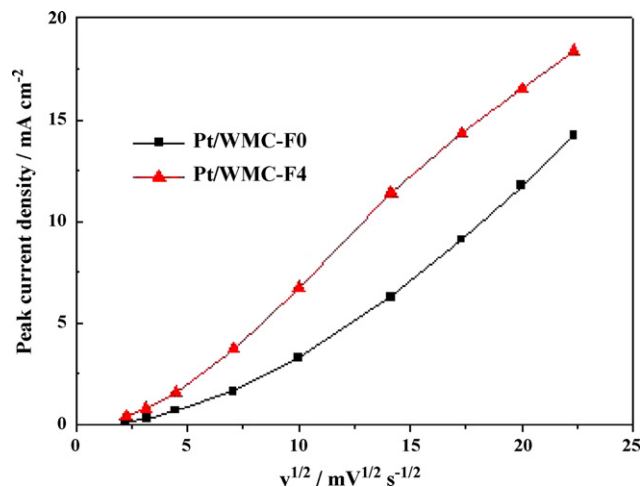


Fig. 3. Plots of the anodic peak current density against the square-root of the scan rate for the hydrogen electrooxidation on Pt/WMC-F0 and Pt/WMC-F4 in 0.1 mol L<sup>-1</sup> HClO<sub>4</sub>.

This suggests that the pore diameter of WMCs has a decisive effect on the electrochemical surface area and Pt utilization.

Fig. 2(b) gives the hydrogen electrooxidation polarization curves for Pt/WMC-F0 and Pt/WMC-F4, obtained in H<sub>2</sub> saturated 0.1 mol L<sup>-1</sup> HClO<sub>4</sub> at a scan rate of 10 mV s<sup>-1</sup> with the rotation speed of 1600 rpm. Along with the potential increment, the corresponding current increases significantly and reaches a limiting value. By comparing these two curves, it can be clearly seen that Pt/WMC-F4 displays higher current density than Pt/WMC-F0.

For the investigation of the pore diameter effect of WMCs on the mass transportation, the relationship between the peak current density ( $I_p$ ) and the square-root of the scan rate ( $\text{mV s}^{-1}$ )<sup>1/2</sup> for hydrogen electrooxidation over Pt/WMC-F0 and Pt/WMC-F4 is plotted and displayed in Fig. 3. One can distinguish that, in both cases, there is an approximately linear  $I_p \propto v^{1/2}$  relationship, typical of an electrochemical reaction under diffusion control. The obvious bigger peak current density at various scan rates features the higher activity of hydrogen electrooxidation over Pt/WMC-F4 with respect to Pt/WMC-F0.

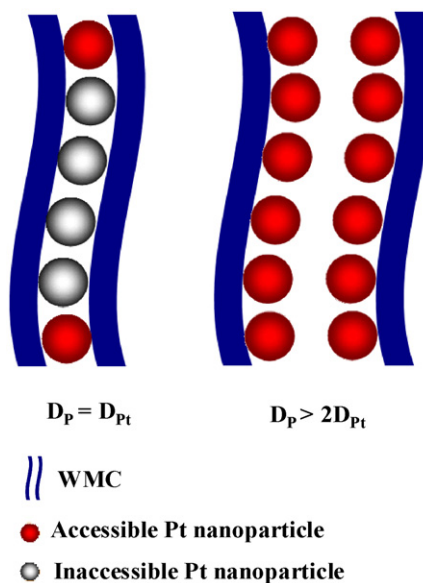


Fig. 4. A scheme of the effect of pore diameter of WMCs support materials on the accessibility of Pt nanoparticles.

These above results can be explained as follows (see Fig. 4): In the case of Pt/WMC-F0, the diameter of Pt nanoparticles is just equal to carbon support WMC-F0's pore size, as a result of which, the two Pt nanoparticles at both top and bottom of every pore will block the pore and thus the inner Pt nanoparticles in this pore will be inaccessible to both electrolyte and reactant ( $H_2$ ). Without doubt, Pt nanoparticles in such a carbon support will have very low electrochemical surface area as well as Pt utilization, thus leading to inferior hydrogen electrooxidation activity. In the other case of Pt/WMC-F4, the pore diameter is more than twice Pt nanoparticles. As a result, the Pt nanoparticles supported on each side of pores are unable to contact each other, and in this way the aforementioned pore blockage will not occur in this case of  $D_p > 2D_{Pt}$ , resulting in the excellent accessibility of Pt nanoparticles. This consequently gives much larger electrochemical surface area and much higher Pt utilization efficiency, thus leading to superior hydrogen electrooxidation activity.

#### 4. Conclusions

Based on the above results, it can be concluded that the different pore diameter of WMCs displays a significant effect on the accessibility of Pt nanoparticles. In the case of  $D_p = D_{Pt}$ , Pt nanoparticles have poor accessibility, resulting in very small electrochemical surface area, very low Pt utilization efficiency, and inferior hydrogen electrooxidation activity. Comparatively speaking, in the case of  $D_p > 2D_{Pt}$ , the accessibility of Pt nanoparticles can be greatly increased, and thus, both the electrochemical active surface area and Pt utilization are significantly enhanced. This consequently improves the hydrogen electrooxidation activity. Considering that

supported catalysts have been widely used in modern chemical engineering and scientific research, we hope that the concept introduced in this paper can be further extended to other porous support materials for loading various metal nanoparticles other than Pt.

#### Acknowledgements

This work has been supported by the grant from Hi-Tech Research and Development Program of China (2009AA05Z110), the Project of NSFC (50632040, 50802116, 20903122), the Specialized Research Fund for the Doctoral Program of Higher Education (20070558062, 20080551014), and the Natural Scientific Foundation of Guangdong Province (8451027501001421).

#### References

- [1] D. Zhao, B.Q. Xu, *Angew. Chem. Int. Ed.* 45 (2006) 4955–4959.
- [2] S. Song, Y. Wang, P.K. Shen, *J. Power Sources* 170 (2007) 46–49.
- [3] B.M. Babić, L.M. Vračar, V. Radmilović, N.V. Krstajić, *Electrochim. Acta* 51 (2006) 3820–3826.
- [4] F. Alcaide, G. Álvarez, O. Miguel, M.J. Lázaro, R. Moliner, A. López-Cudero, J. Solla-Gullón, E. Herrero, A. Aldaz, *Electrochem. Commun.* 11 (2009) 1081–1084.
- [5] D. He, L. Yang, S. Kuang, Q. Cai, *Electrochem. Commun.* 9 (2007) 2467–2472.
- [6] Z. Jiang, J. Chen, J.Y. Lee, *J. Power Sources* 184 (2008) 344–347.
- [7] A.D. Taylor, R.C. Seko, J.M. Kizuka, S. D'Cunha, C.M. Comisar, *J. Catal.* 259 (2008) 5–16.
- [8] S.D. Thompson, L.R. Jordan, M. Forsyth, *Electrochim. Acta* 46 (2001) 1657–1663.
- [9] J. Zhou, J. He, G. Zhao, C. Zhang, T. Wang, X. Chen, *Electrochem. Commun.* 10 (2008) 76–79.
- [10] D. Wu, Z. Li, Y. Liang, X. Yang, X. Zeng, R. Fu, *Carbon* 47 (2009) 916–918.
- [11] G. Tamizhmani, J.P. Dodelet, D. Guay, *J. Electrochem. Soc.* 143 (1996) 18.
- [12] W. Li, W. Zhou, H. Li, Z. Zhou, B. Zhou, G. Sun, Q. Xin, *Electrochim. Acta* 49 (2004) 1045–1055.